**Review**

# Magma Movement from the Deep to Shallow Sakurajima Volcano as Revealed by Geophysical Observations

Masato IGUCHI[*]

Studies on the supply system of magma and its behavior based on seismic and geodetic observations are reviewed for recent volcanic activity of the Sakurajima volcano, where three characteristic types of eruptions occurred in the 20th century: the 1914 gigantic flank eruption; the 1946 minor flank eruption; and frequent vulcanian eruptions at the Minamidake summit crater, continuing from 1955 for more than 50 years. The magma plumbing system of Sakurajima is approximated by a deep ($\sim$10 km) magma reservoir beneath the Aira caldera, a shallow reservoir (3-6 km) beneath the central cones, and a conduit connecting the shallow reservoir to the summit crater. From the inflation-deflation pattern and intensity of the vertical displacement, it is estimated that magma has been supplied to the deep reservoir at a rate of $10^7$ m$^3$/year. The shallow reservoir is inferred from vertical displacements, a tilt vector showing the crater side up before the vulcanian eruptions, and an anomalously attenuated zone of seismic waves. The magma migrated from the deep reservoir to the shallow reservoir before the increase in vulcanian eruptivity at the Minamidake crater, as demonstrated by the relocation of the upheaval center of the ground deformation. The increase in seismicity of A-type earthquakes and the migration of their hypocenters toward the shallow part also support the migration of magma. The hypocenters of B-type earthquakes and explosion earthquakes with volumetric sources are concentrated beneath the crater. The hypocenters of A-type earthquakes generated by shear fractures surround the origins of B-type earthquakes and explosion earthquakes. The separation of the hypocenters indicates the existence of a volcanic conduit connecting the shallow reservoir to the bottom of the summit crater. The intrusion of magma into the conduit and smooth ascent up to the crater bottom induce strombolian eruptions and swarms of B-type earthquakes. The magma at the uppermost part of the conduit becomes a cap rock of the conduit against the following intrusive magma, which generates vulcanian eruptions. Upward tilt of the crater side and extensional strain are observed prior to both strombolian activities and the vulcanian activities that follow and turn into downward and contraction strain, respectively, associated with the eruptions. The volatility of the magma has an important role in vulcanian eruptions, in the formation of a gas pocket at the uppermost part of the conduit, and in sudden outgassing triggered by a pressure decrease in the conduit due to gas leakage.

**Key words** : Sakurajima, Aira caldera, Minamidake, magma reservoir, volcanic conduit

## 1. Introduction

Sakurajima is an andesitic volcano located at the southern edge of the Aira caldera and is formed by the central cones of the Kitadake (northern peak) and the Minamidake (southern peak) and a number of parasitic cones on the flanks (Fig. 1). Historically, the eruptive activity of the Sakurajima volcano is characterized by large flank eruptions and vulcanian eruptions at the Minamidake. The flank eruptions occurred at both sides of the central cones during the periods of 1471-1476 and 1779-1780.

In the 20th century, the Sakurajima volcano was quite active, and three types/scales of eruptive activities were recorded. The 1914 eruption was a flank eruption at two sides of the volcano and was the largest in Japan according to modern volcano observations, which has a history of nearly a century. Fortunately, seismological observation was begun using a Milne-type seismometer installed at Kagoshima Weather Station in 1888 (Yamasato, 2005). This was the first seismometer to be installed near a volcano in Japan. The seismometer recorded precursory earthquakes to the 1914 eruption and the following destructive earthquake (M 7.1; Abe, 1981), which occurred 8 hours after the start of the eruption. Also fortunate for researchers is that the first leveling survey was conducted by the Imperial Military during the period from 1891 to 1895 in south Kyushu. A large amount of ground subsidence around south Kyushu was detected, as indicated by the height difference of the second precise leveling conducted after the eruption (Omori, 1916).

[*] Sakurajima Volcano Research Center of DPRI, Kyoto Univ., Sakurajima-Yokoyama, Kagoshima 891-1419, Japan.

Corresponding author: Masato Iguchi
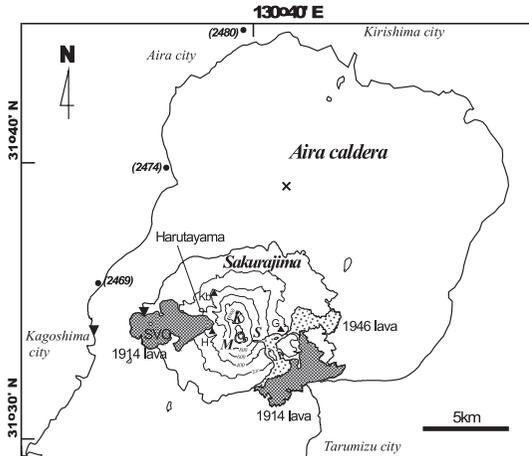e-mail: iguchi@svo.dpri.kyoto-u.ac.jp

Fig. 1. Map of Sakurajima and the Aira caldera. The dots indicate important benchmarks referred to in the text, and the inverted triangles indicate tide gauges. The central cones and craters are *K*: Kitadake, *M*: Minamidake, and *S*: Showa crater. Representative parasitic cones are indicated by triangles (H: Hikinohira, G: Gongen-yama, and Kb: Kabano). Cross represents a pressure source location obtained by Mogi (1958).
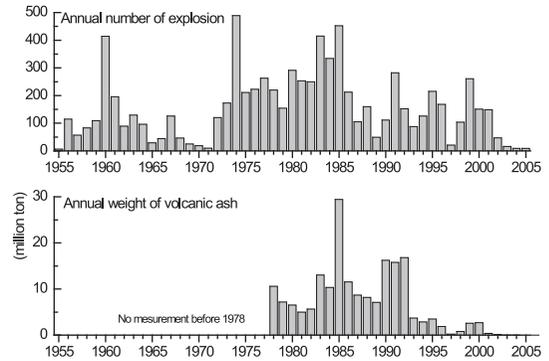


Fig. 2. Annual numbers of vulcanian eruptions and weights of volcanic ash ejected from the Minamidake crater during the period from 1955 to 2005. Observation of weight of volcanic ash started in 1978 by the Kagoshima Prefectural Government.

After the 1914 eruptions, Sakurajima was dormant for some time, but the eruptive activity resumed at the Minamidake summit crater in 1935 and then shifted to a vent at the eastern flank in October 1939. Pyroclastic flows frequently occurred at the eastern crater (Tsuya and Minakami, 1940). Vulcanian eruptions reoccurred at the crater after 1941. In January 1946, explosive eruptions became frequent and lava began to flow out from the single crater on March 9. A number of observations on post-activity were performed by the Earthquake Research Institute of University of Tokyo. For example, the characteristics of volcanic tremors (Nagata *et al.*, 1948) and the physical properties of lava flow (Hagiwara *et al.*, 1948) were investigated. At present, the crater is referred to as the Showa crater.

The most recent eruptive activity was the frequent occurrence of vulcanian eruptions at the summit crater of the Minamidake, which commenced on October 13, 1955 and continued for more than 50 years, producing 7,900 vulcanian eruptions (Fig. 2). The Sakurajima Volcanological Observatory (SVO) was established as an affiliated facility of the Disaster Prevention Research Institute of Kyoto University in 1960 to study the forecast of volcanic eruptions. The magma supply system has been investigated through a combination of seismic and geodetic methods. The National Project of Prediction of Volcanic Eruption, which began in 1974, has promoted the development of an observation system and collaboration among

universities and institutes. Continuous observations have revealed precursory phenomena to the vulcanian eruptions and their mechanisms.

Studies on the magma plumbing system of the Sakurajima volcano, which provides adequate information as a result of the frequent occurrence of volcanic eruptions, are summarized based on observations of the volcano.

## 2. Magma reservoir beneath the Aira caldera

On January 12, 1914, an eruption occurred at the western and eastern flanks (Fig. 1). The eruption was the largest in the 20th century in Japan, and 1.34 km³ of lava and 0.52 km³ of pumice and ash were ejected from the craters (Ishihara *et al.*, 1981). The first leveling survey in south Kyushu was conducted in 1891. After the 1914 eruption, a second leveling survey was conducted and significant ground subsidence was detected all over south Kyushu (Omori, 1916), as shown in Fig. 3. For example, BM2474 (Fig. 1) at the western rim of the Aira caldera subsided by 0.9 m (Omori, 1916). The center of the ground subsidence is not located beneath Sakurajima but rather near the center of the Aira caldera. Mogi (1958) applied a model of the pressure source of a small sphere embedded in a homogeneous half space to the spatial distribution of the vertical displacement, instead of the block movement hypothesis discussed by Tsuboi (1929) and Miyabe (1934). The elastic model applied by Mogi (1958) was first proposed by Yamakawa (1955). The deflation pressure source was estimated to be located at a depth of 10 km near the center of the Aira caldera. This indicates that the magma reservoir, as the origin of the magma product ejected by the 1914 eruption, was not located beneath Sakurajima, but rather beneath the Aira caldera.

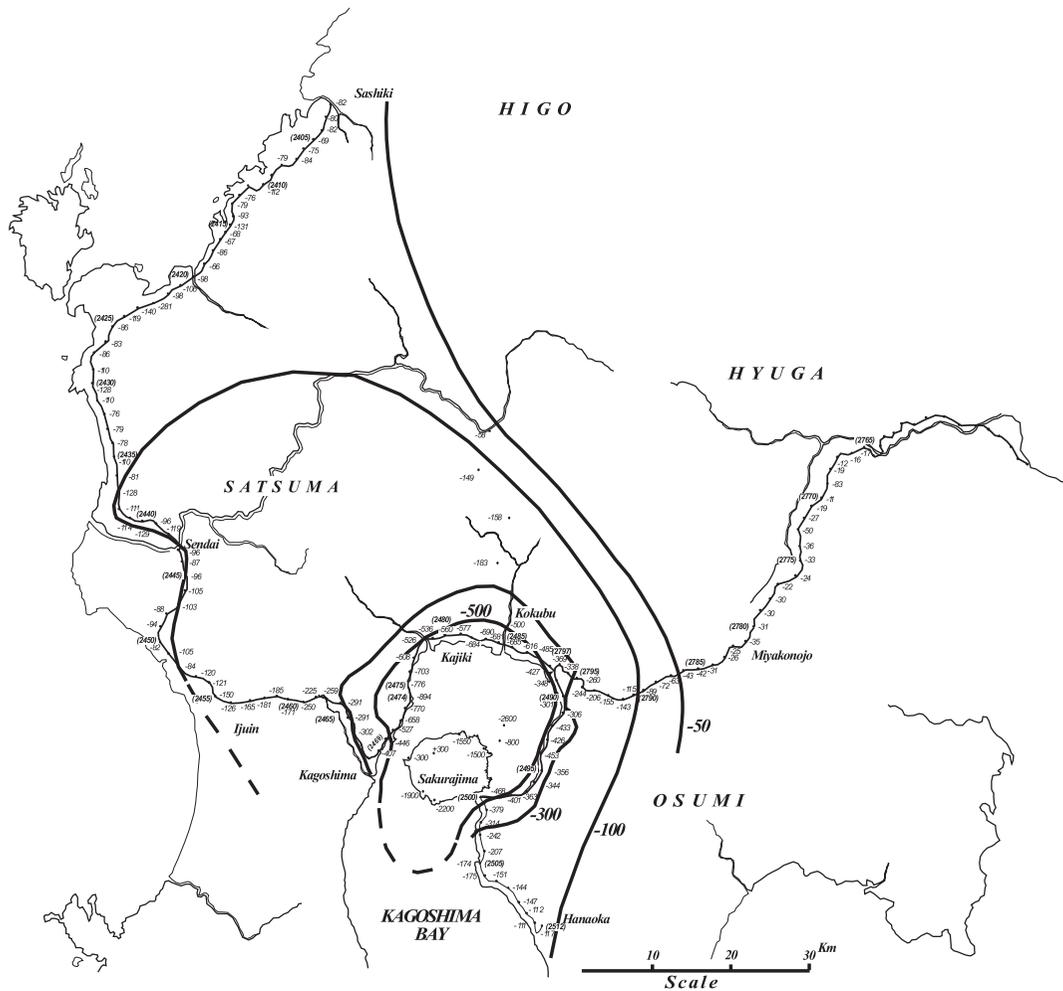Associated with the 1914 eruption, a large amount of

Fig. 3.   Spatial distribution of height difference in south Kyushu before and after the 1914 eruption of Sakurajima (modified from Omori, 1916). Benchmarks are indicated by dots with numbers in brackets, and contours lines indicate isobaths in millimeters.

magma intruded into Sakurajima as observed by uplift near the center of the volcano and extension in the north-south direction. A trigonometric point was uplifted by 0.14 m and the peaks of Hikinohira and Gongen-yama (Fig. 1) were uplifted by 9.7 m and 10.4 m, respectively. Horizontal displacements were quite large and ranged from 1 to 4.5 m (Omori, 1916). Yokoyama (1986) proposed a model composed of two $P_1^0$ (cos $\theta$) sources at depths of approximately 2 km (beneath the volcano) and 8 km, which is an oblique pressure source resulting in an asymmetric depression around the Aira caldera. Hashimoto and Tada (1988) proposed a composite model of a deflation source beneath the Aira caldera and a tensile fault in Sakurajima.

The ground around the Aira caldera has been uplifted since 1916 (Fig. 4). As a result of the eruption at the

Showa crater located at the eastern flank of the Minami-dake (Fig. 1), 0.18 km³ of lava was effused (Ishihara *et al.*, 1981). The ground around the Aira caldera is estimated to have subsided by approximately 10 cm (Sassa, 1956). However, uplift of the ground resumed after the 1946 eruption.

Moreover, the ground deformation is closely related to eruptive activity at the Minamidake crater during the period from 1955 to 2009. Fig. 2 shows the annual numbers of explosive eruptions and the annual amounts of volcanic ash ejected from the crater. Explosive eruptions are defined by the SVO according to the intensity of the explosion ($\geq 10 \mu$m) and the air-shock ($\geq 10$ Pa) at Haruta-yama, which is located 2.7 km from the crater (Fig. 1). The amounts of volcanic ash are estimated from the

monthly weights of ash deposit at 58 sampling points in south Kyushu (Ishikawa *et al*., 1981). Before 1973, the annual number of explosive eruptions was less than 200, except for 1960, and the ground around the Aira caldera continued to be uplifted (Figs. 4 and 5). Eruptive activity significantly increased after 1974. The annual number of explosive eruptions ranged from 200 to 400, and the

annual weight of volcanic ash ranged from $1 \times 10^7$ to $3 \times 10^7$ tons during the period from 1974 to 1992. During the period of enhanced activity, uplift of the ground around the Aira caldera suspended or changed to subsidence (Fig. 5).

Analyzing the vertical displacement during the period of lower eruptive activity in 1957 and 1958, Yoshikawa (1961) found an inflation source at a depth of 10 km beneath the center of the Aira caldera, where the depression source was located for the 1914 eruption (Mogi, 1958). Similarly, a deflation pressure source occupied the same position during the highly eruptive period starting from 1974 (Eto and Nakamura, 1986). Note that the main pressure source stably exists at a depth of 10 km beneath the Aira caldera, and the inflation and deflation of the pressure source is closely related to the eruptive activity, i. e., inflation for the case of low eruptivity and deflation for the case of high eruptivity. Therefore, it is inferred that the pressure source corresponds to the main magma reservoir beneath the Aira caldera. The existence of the magma reservoir is supported by strongly attenuated seismic waves, which propagate under the Aira caldera (Ono *et al*., 1978).

The explosive activity of Sakurajima declined after the peak in 1985, when the annual number of explosive eruptions reached 452 (Fig. 2). Corresponding to a gradual decrease in eruptivity, the subsidence ground deformation changed to uplifting around 1993 (Fig. 5; Eto *et al*., 1997; Eto *et al*., 1998a). The ground at the northern part of
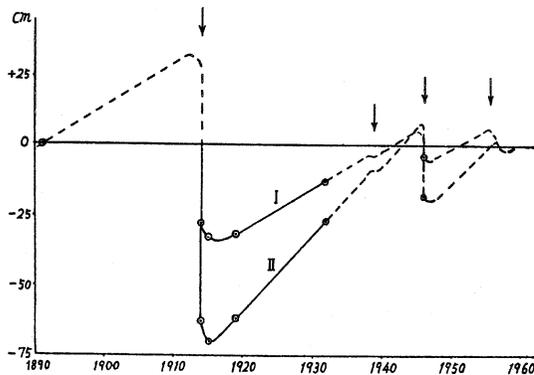


Fig. 4. Secular change in vertical displacement after the 1914 eruption (Sassa, 1956) I: BM2480, II: BM2474. See the locations of the benchmarks in Figs. 1 and 3. The dashed curves indicate estimations, and eruptions are indicated by arrows.
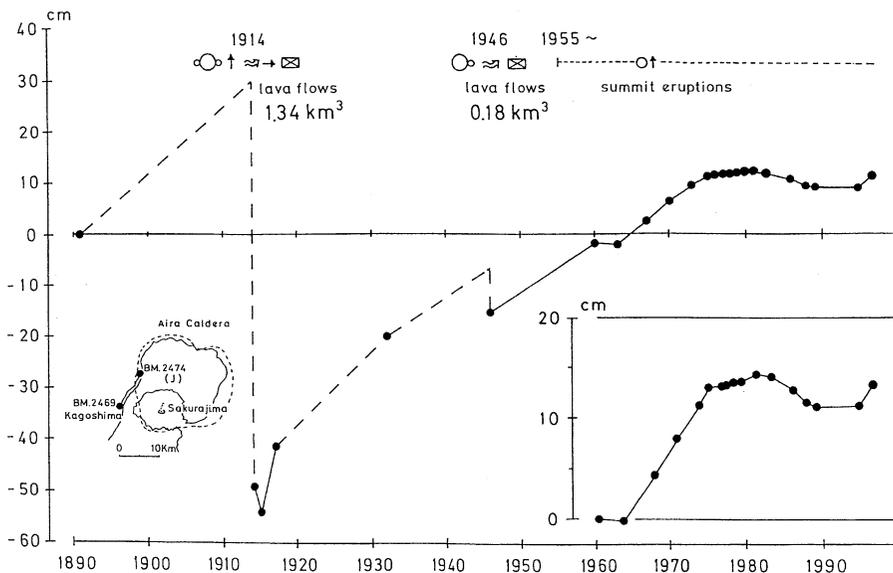


Fig. 5. Secular changes in the relative heights of BM.2474 referring to BM.2469 and the volcanic activity at Sakurajima (Eto *et al*., 1997). The vertical displacement after 1960 is enlarged in a square in the lower-right corner. The dashed lines indicate an estimation based mainly on Sassa (1956). The volumes of the lava flows effused by the 1914 and 1946 eruptions are $1.34 \, km^3$ and $0.18 \, km^3$, respectively.
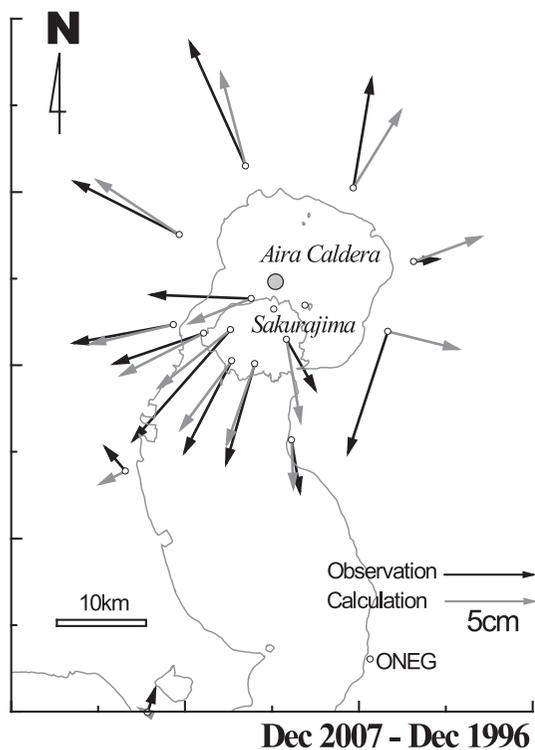
Fig. 6.  Horizontal displacement vectors during the period from December 1996 to December 2007 (Iguchi *et al*., 2008a). The solid and gray arrows show the observation and calculated vectors, respectively. The gray circle indicates the location of the Mogi pressure source. Station ONEG is used for reference.

Sakurajima was uplifted by 12 cm during the period from 1993 to 2009 (Yamamoto *et al*., 2010). Similarly, an EDM survey revealed the start of extension of a baseline across the Aira caldera around 1992−1993 (Eto *et al*., 1998b). Clear extension of the ground around the Aira caldera was confirmed by GPS measurement, revealing radially outward displacements from the center of the caldera (Fig. 6; Iguchi *et al*., 2008a; Kriswati and Iguchi, 2003). Analyzing the horizontal displacements from 1996 to 2007, a Mogi type pressure source (Mogi, 1958) is estimated to be located at a depth of 11 km beneath the center of the Aira caldera and the volume increase is estimated to be $8 \times 10^7$ m$^3$ (Iguchi *et al*., 2008a). This implies that the magma reservoir is located beneath the Aira caldera and that the volume of magma has increased since 1993. The amount of magma continues to grow in 2011.

The magma supply rate is estimated from the addition of volume change of the pressure source inducing the ground deformation and the magma volume equivalent to the volcanic product ejected from the crater. Ishihara (1981) analyzed the vertical displacements measured by repeated

precise leveling to estimate the average magma supply rate to the magma reservoir beneath the Aira caldera after the 1914 eruption. The average rate was obtained as $1 \times 10^7$ m$^3$/year. Continuous GPS observation since 1995 has revealed a temporal change in the magma supply rate. The magma supply rate increased to $2 \times 10^7$ m$^3$/year during the periods from November 1997 to October 1999 and October 2004 to February 2005. However, the average rate was $1 \times 10^7$ m$^3$/year (Iguchi, 2006). It is estimated that $1.4 \times 10^8$ m$^3$ of magma has been newly supplied during the period from 1993 to 2011.

### 3.  Magma reservoir beneath central cones

The SVO has conducted leveling surveys in the Sakurajima area since the first stage of eruptive activity at the Minamidake from 1955. A dual-pressure source model was proposed by adding a minor source beneath Sakurajima to the major source beneath the Aira caldera. Minor pressure sources are estimated to be located at a depth of 3 km in the inflation stage (Yoshikawa, 1961), and the depth is determined to be in the range of from 2 to 6 km in the deflation stage after 1974 (Fig. 7; Eto and Nakamura, 1986). Inflations and deflations of the major pressure source are closely related to the eruptive activity, and the pressure source corresponds to the magma reservoir beneath the Aira caldera. Therefore, the minor pressure source corresponds to a supplementary magma reservoir beneath the Minamidake crater.

The existence of a supplementary magma reservoir is confirmed by tilt and strain changes associated with explosive eruptions at the Minamidake crater and strong attenuation of seismic waves propagating below the Minamidake. The crater-side-up tilt and the extension strain are observed 10 minutes to several hours before the explosive eruptions and changed into crater-side-down tilt and contraction strain, respectively, after the start of the explosions (Kamo and Ishihara, 1989). The inflation and deflation tilt vectors are oriented approximately in the direction of the Minamidake crater, and the inflation and deflation sources are located at depths of from 2 to 6 km (Ishihara, 1990).

S-waves propagating at depths of 3 to 6 km beneath the central cones experienced strong attenuation (Kamo *et al*., 1980). The amplitudes of P-wave first motion coming from the direction of the crater are significantly smaller, by one to two orders of magnitude (Suzuki, 1999). Such a highly attenuated zone has an extent of 2 to 3 km. In addition, the region of 3 to 6 km in depth is an aseismic zone of the A-type earthquake (Fig. 8).

### 4.  Migration of magma from the Aira caldera toward Sakurajima

Volcanic earthquakes at the Sakurajima volcano are classified as A-type and B-type earthquakes, explosion earthquakes, and tremors, based on Minakami's classifi-
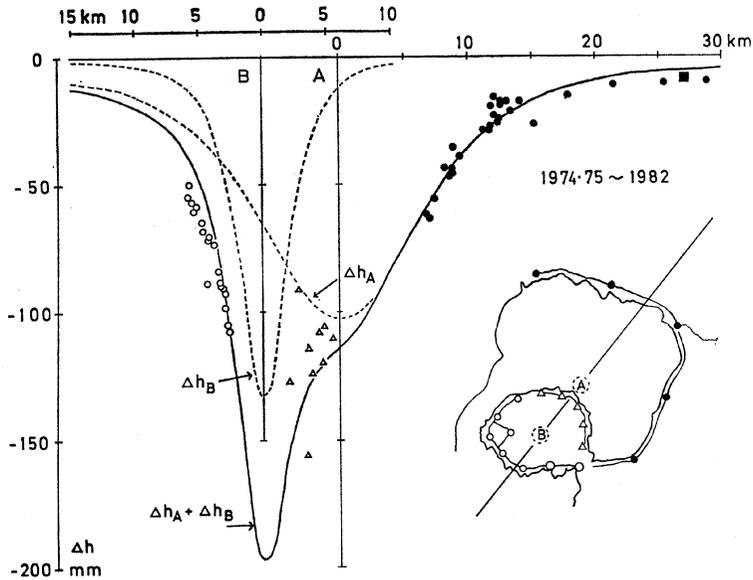
Fig. 7.   Vertical displacement fitted by the theoretical value of sources A and B (Eto and Nakamura, 1986). The depths of sources A and B are 10 km and 3 km, respectively. The dashed curves $\Delta h_A$ and $\Delta h_B$ indicate the displacements induced by individual sources A and B, respectively, and the solid curves are the sums of $\Delta h_A$ and $\Delta h_B$ on the line passing through sources A and B. The dots, triangles, and open circles indicate the vertical displacements at the east and north rims of the Aira caldera, at the south and west parts of Sakurajima, and at the east and north parts of Sakurajima, respectively. The locations of the benchmarks are shown on the map, although some are omitted.

cation criteria (Minakami, 1974).  A-type earthquakes belong to the same category as volcano-tectonic earthquakes having distinct P- and S-phases. B-type earthquakes are characterized by the dominance of lower-frequency content and ambiguous phases. B-type earthquakes are categorized as BH-type and BL-type earthquakes according to the dominant frequency (BH-type: 4–7 Hz and BL-type: 1–3 Hz; Iguchi, 1989). Explosion earthquakes are associated with vulcanian eruptions and have larger amplitudes and lower-frequency content than B-type earthquakes. Volcanic tremors are classified as spasmodic tremors with continuous volcanic ash emission and harmonic tremors, which are referred to as C-type earthquakes, at Sakurajima (Kamo *et al.*, 1977).

Transitions of volcanic earthquake types suggest the ascent or migration of magma.  In March 1976, an A-type earthquake occurred at a depth of grater than 10 km SSW of Sakurajima, and the hypocenter became shallower and approached the summit (Fig. 8).  The seismicity changed to swarms of B-type earthquakes in May, and the activity of the vulcanian eruptions then increased.  The migration of hypocenters of A-type earthquakes was interpreted to correspond to the upward migration of magma (Kamo, 1978).

The spatial distribution of the vertical ground deformation revealed the relocation of a pressure source, related to

the eruptive activity.  Ishihara and Eto (1978) revealed the transition of the spatial pattern of the vertical displacement, as shown in Fig. 9.  The pressure source remained at the center of the Aira caldera, and Sakurajima exhibited an upward tilt of the north side in the first period.  The pattern may continue from the beginning of the eruptive activity at the Minamidake crater in 1955.  The second period corresponds to transition of activity from low eruptivity to higher eruptivity from September 1972.  The entirety of Sakurajima was uplifted, and the center of uplift migrated to the northern part of the island.  Either magma migrated to Sakurajima from the center of the Aira caldera or a secondary magma reservoir was formed beneath Sakurajima.  When eruptive activity was maintained at a high level after 1974, the ground in and around Sakurajima exhibited minor depression due to excess discharge of magma product.

Considering migrations of hypocenters of A-type earthquakes SSW of Sakurajima and pressure source at the northern part of the island, Kamo (1988) proposed a dual-path model for magma supply to Sakurajima based on both seismological and geodetic observation (Fig. 10c).  The magma reservoirs are inferred to exist at a depth of 10 km beneath the Aira caldera and at a depth of 5 km beneath the Minamidake.  The main path of the magma to the reservoir beneath the Minamidake runs from the reservoir beneath
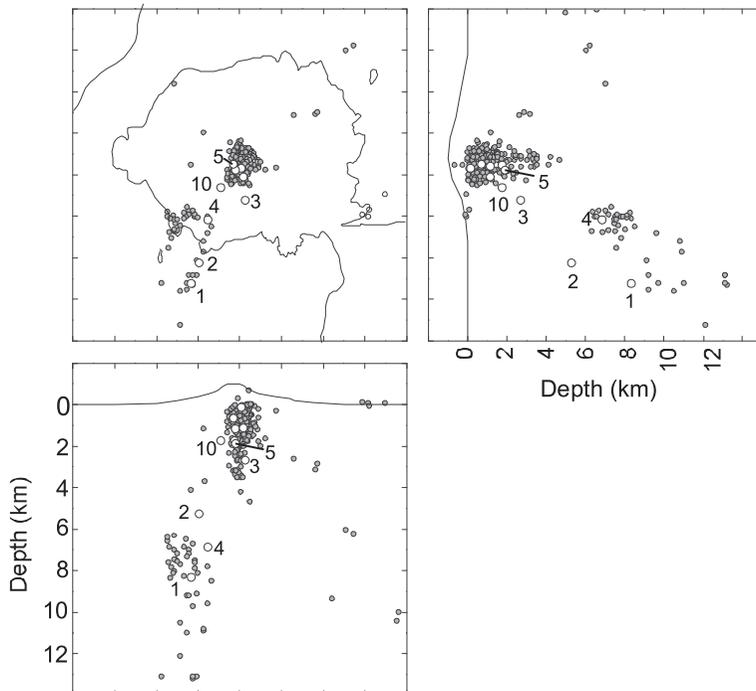
Fig. 8. Hypocenter distribution of A-type earthquakes during the period from 1976 to 2004. The numbered white circles represent the hypocenter location as determined by Kamo (1978) and indicate the order of earthquake occurrence prior to the increase in eruptive activity in May 1976. The numbers 6 through 9 are omitted in order to avoid congestion. These hypocenters are located at depths of less than those of events 5 and 10 beneath the Minamidake.

the Aira caldera. An additional path from the SW part directly to the reservoir beneath the Minamidake was occasionally active. However, Hidayati *et al*. (2007) proposed a single-path model (Figs. 10a and 10b). The magma stored in the reservoir beneath the Aira caldera moved laterally southwestward through a tensile fault striking from NE to SW below the Minamidake, and the seismicity of A-type earthquakes SSW of Sakurajima is interpreted to be due to the concentration of strain at the tip of the tensile crack. The hypocenter distribution SSW of Sakurajima did not exhibit migration in November 2003 and was concentrated at depths of from 6 to 9 km. The focal mechanisms of the events are normal fault type mechanisms, striking NNE to SSW as suggested by the tensile fault direction. No significant ground deformation was detected at the SSW part of Sakurajima during the high-seismicity period. The model proposed by Hidayati *et al*. (2007) may simply explain both seismicity and ground deformation. However, the application of the dual-source model of the tensile fault and the Mogi source to the deformation in the inflation stage after 1993 has not been confirmed. The Mogi source was assumed to be located northeast of Sakurajima in the model, based on the vertical displacement in the deflation stage (*e.g.*, Eto and Nakamura, 1986). However, the inflationary Mogi source after 1993 is obtained north of Sakurajima by both vertical (Eto *et al*., 1998a; Yamamoto *et al*., 2008) and horizontal displacements (Iguchi *et al*., 2008a).

## 5. Conduit beneath the Minamidake crater

The hypocenter distribution of the various types of earthquakes provides an image of the structure of the conduit connecting the magma reservoir beneath the central cone with the summit crater. Fig. 11 shows the hypocenter distribution of A-type, BH-type, and BL-type earthquakes and explosion earthquakes (Iguchi, 1994). The hypocenters of the BH-type and BL-type earthquakes and the explosion earthquakes are concentrated within a radius of 200 m beneath the crater at depths of 1 to 3 km. In contrast, the hypocenters of the A-type earthquakes are not located within the zone of the BH-type and BL-type earthquakes and explosion earthquakes, but rather surround it. A-type earthquakes are generated by shear faulting of rock. Therefore, the surrounding zone is brittle. On the other hand, the moment tensors of the source for B-type earthquakes and explosion earthquakes exhibit a volumetric increase that is dominated by a non-double couple component (Iguchi, 1994; Tameguri *et al*., 2002). In addition,
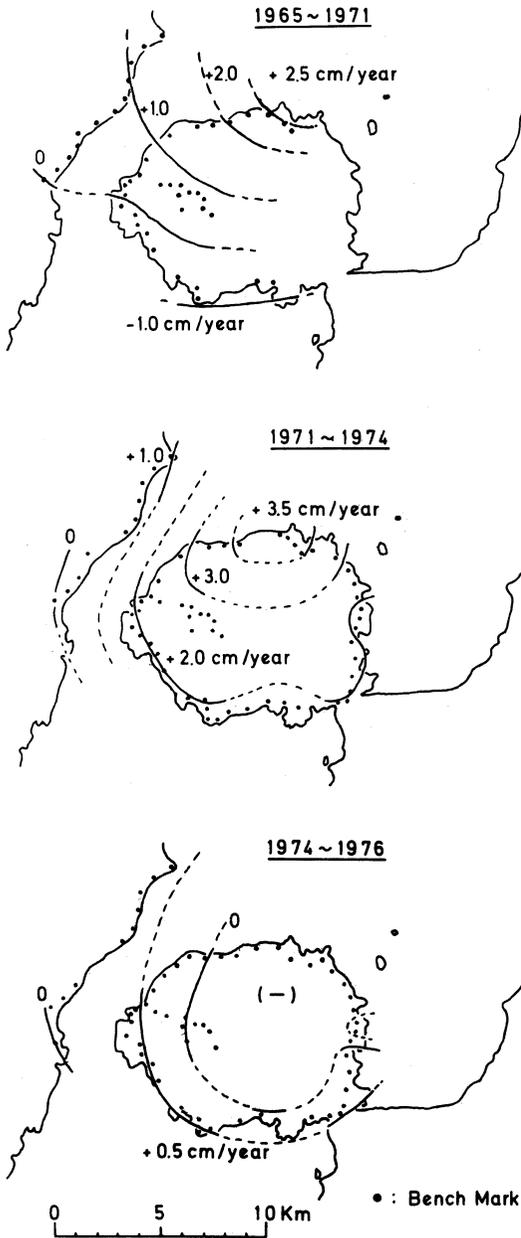
Fig. 9. Distribution of vertical displacement in three periods (Ishihara and Eto, 1978). The displacement is in reference to BM.2469 (Fig. 1), and the elevation at Sakurajima is connected by the tide difference between two ports: Kagoshima and Hakamagashi in Sakurajima (see Fig. 1). Top: the vertical displacements at the northern part are maximal. Middle: the entirety of Sakurajima is uplifted higher than Kagoshima. Bottom: the number of explosive eruptions increased. Ground deformation revealed no uplift or subsidence, particularly at the NE part.

BL-type earthquakes and explosion earthquakes are associated with strombolian and vulcanian eruptions, respectively. Therefore, it is inferred that both BL-type earthquakes and explosion earthquakes occur in the fluid-filled conduit. The separation of the hypocentral zone suggests that the magma-filled conduit is distinguishable from the solid rock (Iguchi, 1994). The radius of the conduit is estimated to be 200 m at a depth of from 2 to 3 km. However, the radius of the upper part of the conduit is 40 to 60 m (Ishihara, 1990). The radius of conduit decreases as the shallowness increases.

B-type earthquakes at the Sakurajima volcano sometimes swarm from one to a few days before the number of vulcanian eruptions increases (*e.g.*, Nishi, 1984). However, the occurrences of the BH-type and BL-type earthquakes correspond to different stages of magma intrusion into the conduit. The hypocenters of the BL-type earthquakes are distributed at depths of from 1 to 3 km below the crater, which is similar to the hypocenters of the explosion earthquakes. The hypocenters of the BH-type earthquakes are located at greater depths of 2 to 3.5 km (Fig. 11). The ground deformations and surface phenomena at the crater during the occurrence of swarms of BH-type and BL-type earthquakes exhibit significant contrast. When BL-type earthquakes swarm, crater-side-down tilt and contraction strains associated with eruptive activity of strombolian eruption or andesitic fountain at the crater were observed (Fig. 12a; Ishihara and Iguchi, 1989). The deflationary ground deformation is caused by the emission of volcanic ash and gas from the crater. Successive occurrence of BH-type earthquakes is associated with crater-side-up tilt (Fig. 12b) and extensional strain, but is accompanied by only weak fumarolic activity. BH-type earthquakes are believed to have been generated by the intrusion of magma into the lower part of the conduit. Moreover, BL-type earthquakes are associated with the ascent of magma to the bottom of the crater, and effusion of the magma is associated with significant degassing.

Tateo and Iguchi (2009) detected upward tilt of the crater side and extensional strain before the occurrence of BL-type earthquake swarms. Inflations begin 2 to 20 hours before the commencement of BL-type swarms. The durations of these inflations are longer and the deformation rates are smaller than those of the ground deformation immediately before the occurrence of vulcanian eruptions (Fig. 13). The inflation source is located at a depth of 4 km below the Minamidake crater. This indicates that inflation before BL-type earthquake swarms is a process of magma intrusion into the upper part of the conduit and the ascent of the magma head approaching the ground surface. The rate of inflation associated with a BH-type earthquake swarm is as large as the maximum level of the inflation rate before BL-type earthquake swarms. The intrusion of magma at a high rate induces a BH-type earthquake swarm, which then changes to a BL-type earthquake
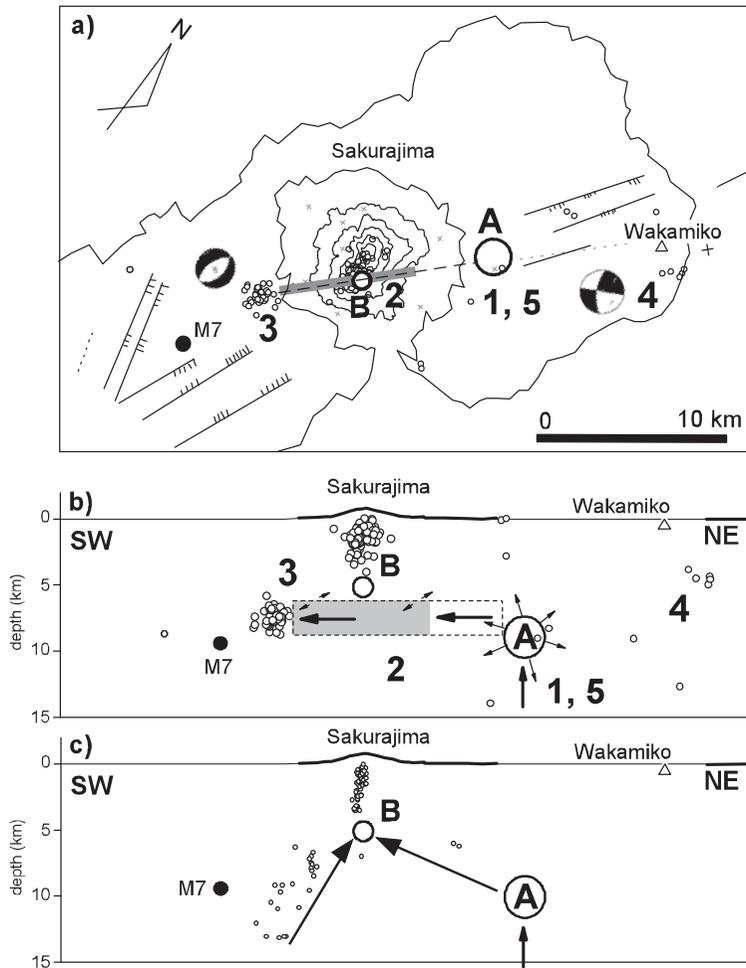
Fig. 10.    Models of magma migration toward the Sakurajima volcano. A hypothetical model of the magma supply system at the Sakurajima volcano. (a) Horizontal plane and (b) vertical cross-section in the SW−NE direction (Hidayati *et al*., 2007). The numbers correspond to volcanic processes during the period from 1999 to 2005. The open circles indicate VT earthquakes. The open circles with "A" and "B" are pressure sources beneath the Aira caldera and Sakurajima, respectively. The tensile fault is indicated by the rectangular dashed line, and the active zone from 2000 to the middle of 2004 is shown in gray. The inferred magma migration is indicated by arrows. The solid circle with M 7 indicates the location of the largest earthquakes for the 1914 eruption as determined by Abe (1981). The lines with branches indicate geological faults, most of which are normal faults. (c) Previous model modified from Kamo (1988). The VT earthquakes that occurred during the period from 1976 to 1980 are plotted.

swarm when the magma reaches the crater bottom.

Based on the lower seismicity of A-type earthquakes (Hidayati *et al*., 2007) and the concentration of hypocenters of explosion earthquakes (Ishihara, 1988) at a depth of 2 km, the conduit is partially enlarged at this depth. The focal mechanism of A-type earthquakes at depths of greater than 2 km exhibit constant strike-slip fault and may be affected by the regional tectonic stress of the N−S extension (Nishi, 1978; Hidayati *et al*., 2007). In contrast, a focal mechanism at a depth of less than 2 km is either a normal or reverse fault mechanism. Typically, the normal fault mechanism is dominant during an increase in explosive activity, and so the mechanism changes to a reverse or strike-slip mechanism when the explosivity decreases (Nishi, 1978). An increase in pressure at a depth of 2 km may cause a tensional stress field above the fault, generating normal fault earthquakes, and a decrease in pressure induces a contraction stress field corresponding to reverse fault mechanism earthquakes (Hidayati *et al*., 2007).
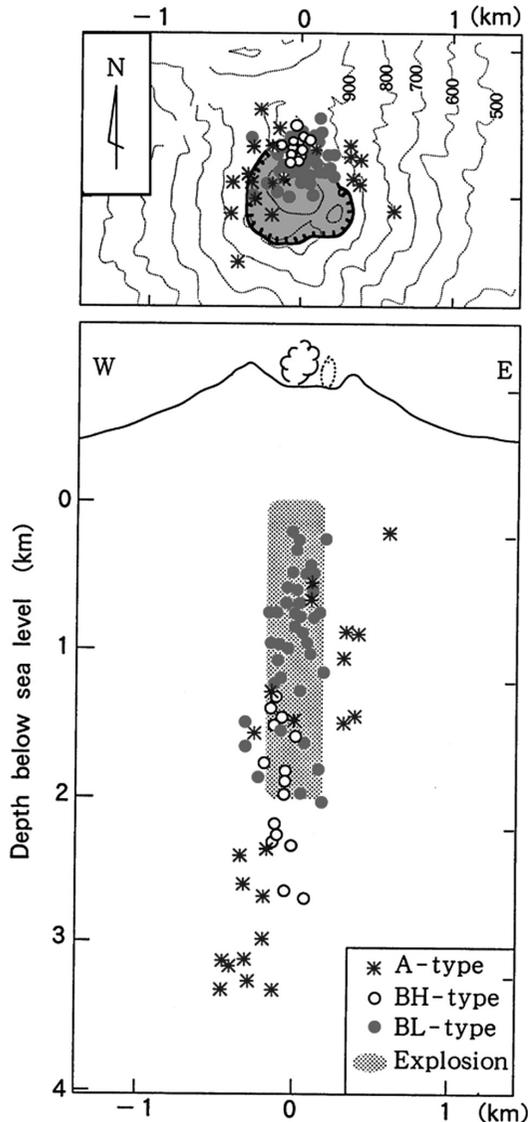
Fig. 11. Hypocenter distribution of A-type, BH-type, and BL-type earthquakes and explosion earthquakes during the period from 1987 to 1988 (Iguchi, 1994). Top: epicenter distribution. Bottom: hypocenter distribution on the cross-section in the east-west direction. The shaded area indicates the hypocentral zone of the explosion earthquakes (Ishihara, 1990)

## 6. Magma movement associated with vulcanian explosion

### 6-1 Preparation process

We believe that a swarm of BL-type earthquakes is a precursor to an increase in explosive eruptions. Uhira and Ueda (1988) investigated the time interval between BL-type earthquake swarms and subsequent explosive erup-

tions. More than 40 % of time intervals were more than 10 days in 1980–1983, whereas 37 % of time intervals were less than one day in 1984–1988. BL-type earthquakes associated with ascent of magma to the crater bottom or effusion of magma from the vent occur. A swarm of BL-type earthquakes, indicating a magma-filled conduit (Iguchi, 1994) might be a precursor to explosive activity. However, it is difficult to explain difference in the time interval between 1980–1983 and 1984–1988, as shown by Uhira and Ueda (1988).

The extension strain and upward tilt of the crater side are detected immediately before the occurrence of explosive eruptions (Kamo and Ishihara, 1989), and this inflation indicates magma intrusion into the lower part of the conduit and the reservoir at depths of from 2 to 6 km (Ishihara, 1990). Nogami *et al*. (2006) analyzed the water-soluble content-attached volcanic gas and found that the molar ratios of $HCl/SO_4$ of volcanic ash ejected by explosive eruptions were lower than those by strombolian eruptivity in the case of a BL-type swarm. This indicates that the explosive eruptions ejected degassed magma. Based on these considerations, two requirements must be satisfied for the explosive eruptions to occur under an open-conduit system during the period of the Minamidake activity. The first requirement is that the upper part of the conduit is plugged by degassed magma. Fresh magma is driven up to the crater bottom, and the magma is degassed by strombolian activity with a BL-type swarm. A lava dome at the bottom of the crater and a gas pocket are formed by the degassed magma before the occurrence of an explosive eruption (Ishihara, 1985). The second requirement is a subsequent intrusion of new magma into the lower part of the conduit. The difference in the time interval from BL-type earthquake swarms to the subsequent explosive eruptions between 1980–1983 and 1984–1988 (Uhira and Ueda, 1988) may be related to the time interval of the intrusion of magma. Magma intrusion frequently occurs in shorter time intervals in 1984–1988, as compared to 1980–1983. As a result, a greater number of BL-type earthquake swarms and explosive eruptions occurred in 1984–1988. When the upper conduit is not occupied by degassed magma, new magma smoothly ascends to the crater bottom, followed by strombolian eruptions and a BL-type earthquake swarm. Successive occurrence of a BL-type earthquake swarm and explosive activity is explained schematically by the interaction of old degassed magma and newly intruded magma (Fig. 14; Tateo and Iguchi, 2009).

The formation of the gas pocket sometimes induces harmonic tremor. The spectrum of the harmonic tremor at Sakurajima is characterized by sharp peaks at frequencies of multiple integers of the fundamental frequency (Kamo *et al*., 1977; Maryanto *et al*., 2008). Nishi (1984) demonstrated that the occurrence of the harmonic tremor after the BL-type earthquake swarm is a more reliable precursor to
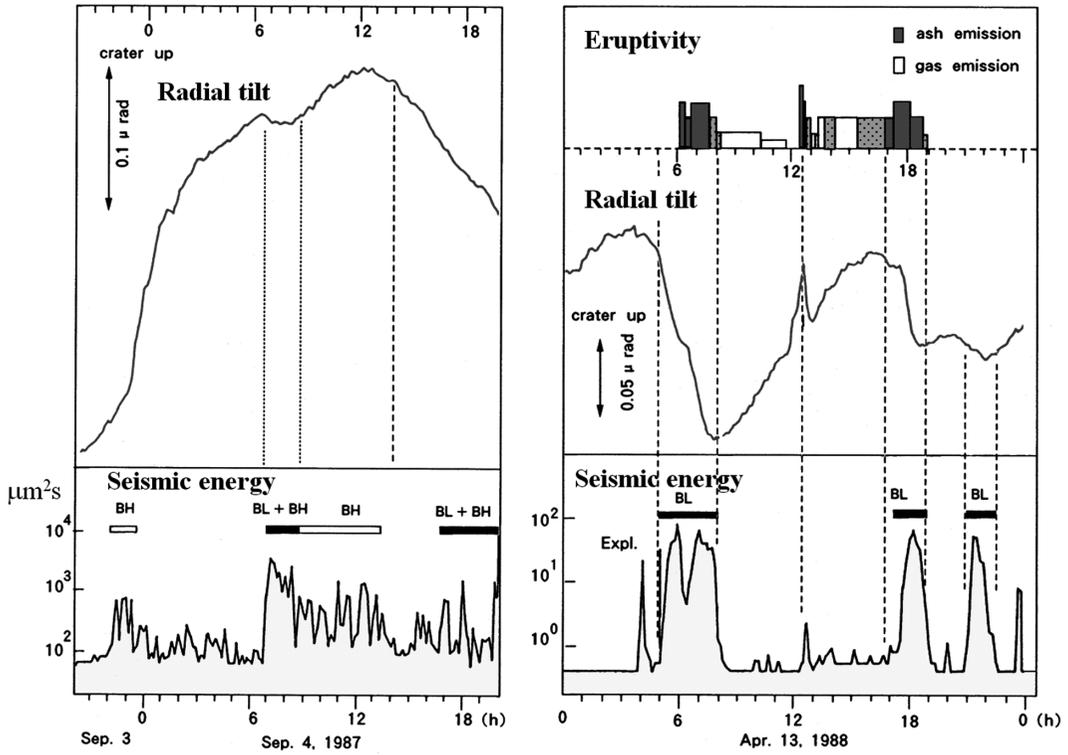
Fig. 12.   Tilt changes associated with swarms of BL-type earthquakes (a) and BH-type earthquakes (b) (modified from Ishihara and Iguchi, 1989). Tilts were observed at the underground tunnel at Harutayama (Fig. 1). (a) The seismic energy at station HIK (Fig. 1), which is 1.7 km from the summit crater, is shown in the lower part of the figure, and the temporal change of the eruptive activity associated with the BL-type earthquake swarm is shown in the upper part of the figure. No significant changes in surface phenomena were detected in the BH-type earthquake swarm.
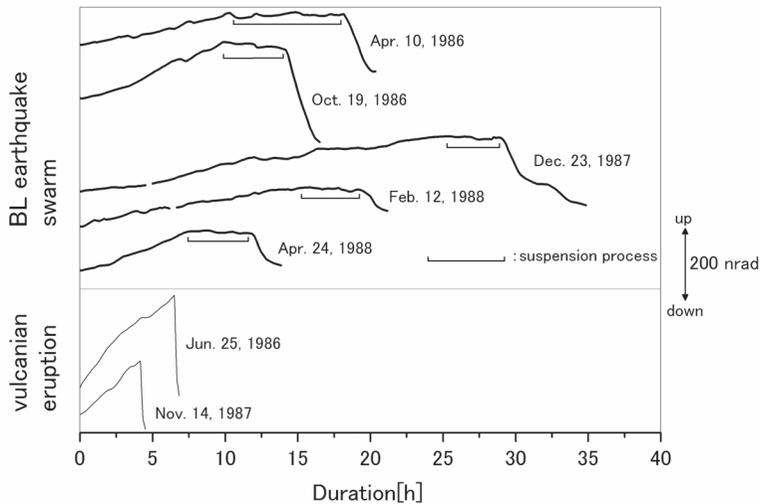


Fig. 13.   Examples of tilt change associated with a BL-type earthquake swarm (upper) and vulcanian eruption (lower). Eruptive activity continued during the downward tilt of the crater side (Tateo and Iguchi, 2009). Tilts were observed at the underground tunnel at Harutayama (Fig. 1). The upward tilt of the crater side changes to downward tilt after a short period of deadlock, as indicated by the suspension process.
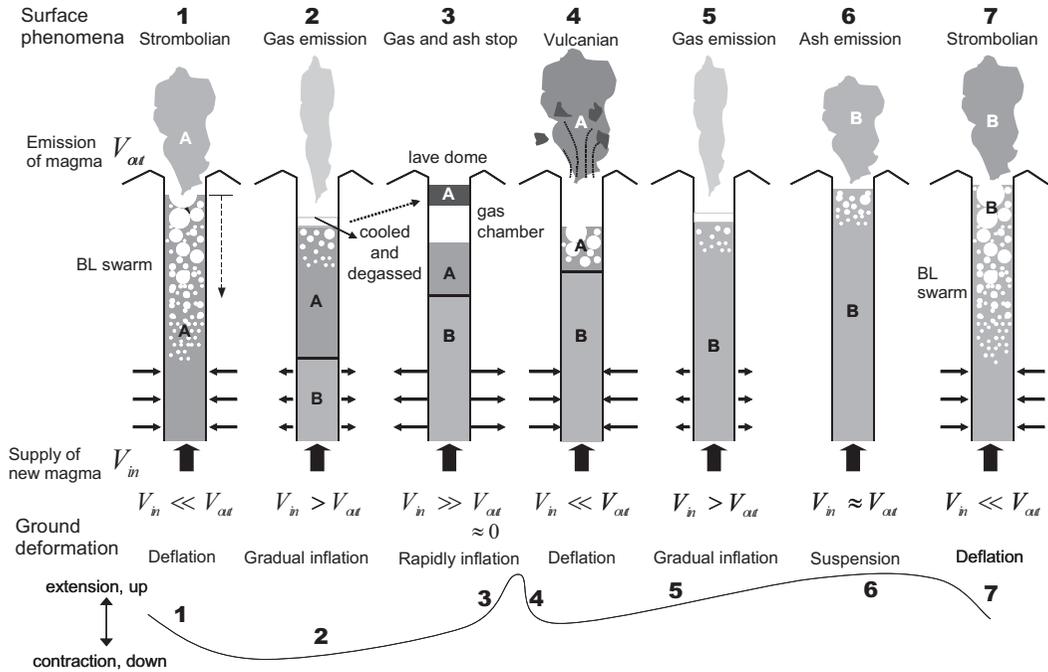
Fig. 14.   Schematic diagram of the internal change of the conduit inferred from ground deformation and surface phenomena (Tateo and Iguchi, 2009). $V_{in}$ indicates the volume of magma supplied from the magma reservoir, and $V_{out}$ indicates the volume of magma emitted as volcanic ash and gas. The symbols "A" and "B" represent magma that was supplied to the conduit in different stages. The inward and outward arrows indicate deflation and inflation of the deep part of the conduit, respectively. Larger volume changes are indicated by larger arrows. A schematic diagram of the ground deformation of tilt and strain changes is shown at the bottom of the figure.

explosive activity.  Harmonic tremor is generated by the resonance of bubbly magma (Maryanto *et al*., 2008) at a depth of from 300 to 500 m (Tameguri *et al*., 2007), which indicates that the formation of a gas pocket composed of bubbly magma has an important role in promoting explosive eruption.

## 6−2   Process of vulcanian eruption

The extension strain and upward tilt of the crater side are detected by extensometers and water-tube tiltmeters immediately before the occurrence of explosive eruptions (Kamo and Ishihara, 1989; Ishihara, 1990). An example of tilt and strain records is shown in Fig. 15.  Since the precursory time is only 10 minutes to several hours, the inflation of ground, indicating intrusion of magma, is directly related to subsequent explosive eruptions.

Iguchi *et al*. (2008b) summarized the process of explosive eruption.  As mentioned in the previous section, the top of the conduit is plugged by a lava dome, and a gas pocket is formed immediately below the plug. The pressure in the conduit increases due to the intrusion of magma (first stage in Fig. 16). As the pressure approaches a threshold of the strength of the plug, the gas in the pocket starts to leak (second stage). The second stage is inferred

from the minor contraction of strain.  The third stage is marked by a transient increase in the volume and pressure of magma as a result of abrupt outgassing of the water-saturated magma due to a decrease in pressure following the second stage. The duration of the second stage thus extends from the beginning of the pressure decrease to the start of outgassing in the water-saturated magma is one to two minutes at Sakurajima.  The fourth stage involves an increase in volume and pressure of the gas pocket at the top of the conduit associated with explosive eruptions starting at the bottom of the crater.  The plug confining the gas pocket is destroyed by the expansion of the gas pocket, resulting in an air shock (propagation velocity: M 1.1−1.4; Ishihara, 1985; Yokoo and Ishihara, 2007) and the ejection of volcanic bombs (initial velocity: approximately 200 m/s; Iguchi *et al*., 1983). In the fifth stage, the deflation of the volcanic conduit occurs as a result of a pressure and volume decrease due to the ejection of volcanic gas and ash.  The deflation stage is separated into sudden contraction at the shallow part and gradual deflation at the deeper part, as shown in 5A and 5B in Fig. 16, respectively.  After destroying the plug confining the gas pocket, the volcanic gas and ash are rapidly ejected, and
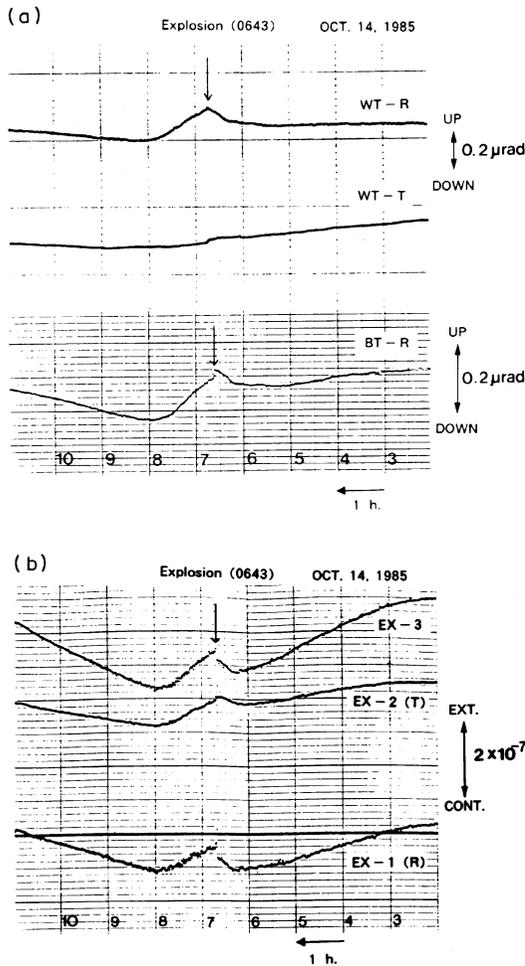
Fig. 15. (a) Tilt and (b) strain changes associated with vulcanian eruption (Ishihara, 1990). (a) "WT-R" and "WT-T" indicate the radial component from the crater and component tangential to the crater, respectively, as recorded by the water-tube tiltmeter in an underground tunnel at Harutayama (Fig. 1). "BT-R" is the radial component of the borehole tiltmeter at a depth of 290 m beneath Harutayama. (b) Extensometer records. EX-1: radial, EX-2: tangential, and EX-3: oblique components in the underground tunnel. The upward tilt of the crater side and the extension strain change started at 8 h.



Fig. 17. An example of velocity seismograms of an explosion earthquake (Tameguri *et al*., 2002). The explosion occurred at 04h55 m, September 3, 1999. "V" is the vertical component of the broadband seismometer, and "R" and "T" represent the horizontal components radial from the crater and tangential to the crater, respectively. "P", "D", and "LP" indicate the characteristic phases of the explosion earthquake. "P" refers to the P-wave first motion with compression onset. "D" refers to the subsequent dilatational P-wave. "LP" refers to the long-period Rayleigh wave.

the gas pocket is collapsed. The deflation gradually proceeds as shown by contraction strain and downward tilt in Fig. 15 at the magma reservoir at a depth of from 2 to 6 km (Ishihara, 1990).

　The third through fifth stages appear as characteristic phases in the explosion earthquake. The third stage is identified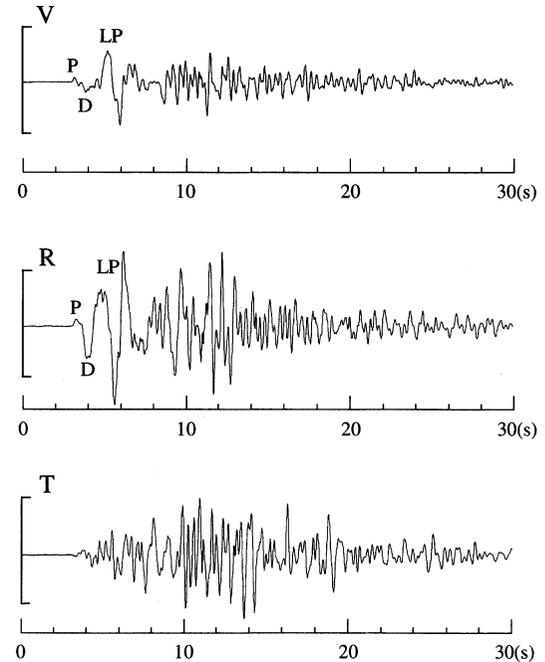 as the onset of explosion earthquakes, the hypocenters of which are located at depths of from 2 to 3 km immediately beneath the Minamidake crater (Nishi, 1976; Yamasato, 1987; Iguchi, 1989; 1994 Tameguri *et al*., 2002). An example of an explosion earthquake is shown in Fig. 17. The P-phase is a compressional P-wave first-motion-generating isotropic expansion, and the subsequent D-phase is a dilatational P-wave that induces cylindrical contraction (Tameguri *et al*., 2002). Moreover, the cylindrical contraction is detected by a longer-period wave (Uhira and Takeo, 1994). The contraction is interpreted to be caused by the upward flow of gas in the conduit. The expansion at a depth of 0.5 km in the fourth stage in Fig. 16 corresponds to an isotropic expansion at the depth, generating the first half of the LP phase composed of a Rayleigh wave (Tameguri *et al*., 2002). More specifically, the cap rock swells as a result of the expansion and is destroyed at the moment of the greatest seismic moment rate of expansion (Yokoo *et al*., 2009). The collapse of the gas pocket at a depth of approximately
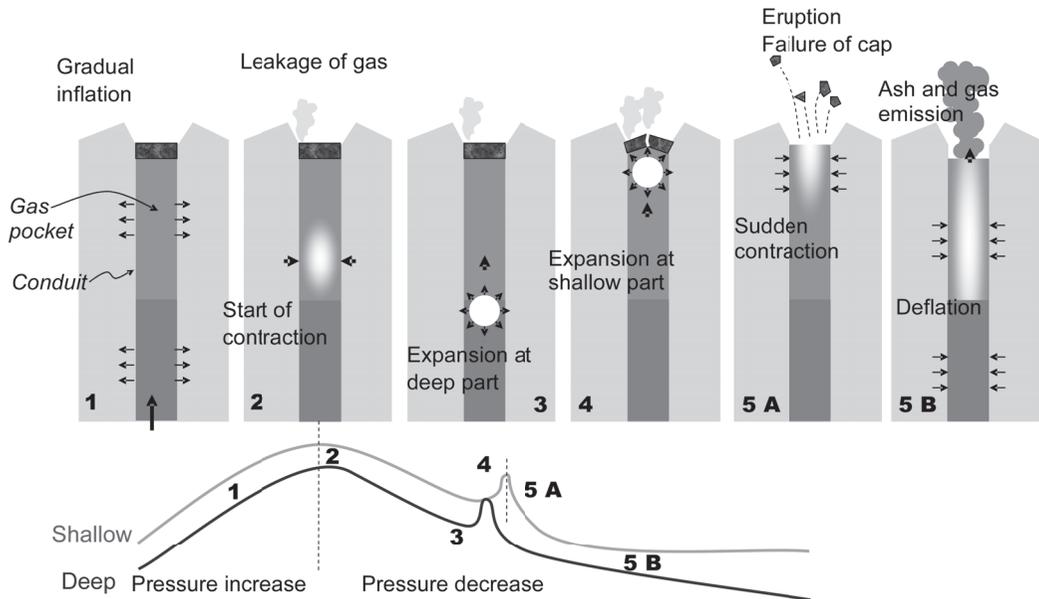
Fig. 16.  Process of explosive eruption based on observations at Sakurajima, Semeru, and Suwanosejima volcanoes (Iguchi *et al*., 2008b). Inferred pressure changes are shown at the bottom. "Shallow" and "Deep" indicate pressure changes at the upper part (less than 0.5 km) and the deep part (approximately 2 km) of the conduit. The difference is recognized at the Sakurajima volcano, and only changes at the shallow parts are detected at Suwanosejima and Semeru volcanoes. (1) Ascent of magma and the accumulation of volcanic gas in the conduit below a confining cap (plug). Pressure and volume increases are observed as inflation-related tilt/strain and upward displacement. (2) Release of gas as the gas pressure exceeds the strength of the cap. The resultant minor contraction is detected as deflation tilt and downward displacement. (3) Pressure decrease in the conduit starting from the gas pocket, inducing sudden outgassing of water-saturated magma deep in the conduit. Expansion is detected by upward P-wave first motion of the explosion earthquake. (4) Expansion process destroying the cap at the top of the conduit. Stages (3) and (4) could not be distinguished at the Suwanosejima and Semeru volcanoes. (5A) Failure of the cap at the top of the conduit. The gas pocket at the upper part of the conduit collapses, inducing a contraction ground deformation source at the shallow part. The deformation is revealed by the step of the crater-side-down tilt and the step of the tensional strain, as well as downward ground deformation. (5B) Ash and gas emission from the conduit. Pressure and volume decreases are observed as deflation-related tilt/strain and downward displacement, respectively.

500 m (stage 5A) is confirmed by the strain step and the step of the crater-side-down tilt (Ishihara, 1990) and the second half of the LP phase generated by the contractive horizontal dipoles (Tameguri *et al*., 2002). This stage is modeled by Kanamori *et al*. (1984) and involves an implosion source and a downward single force acting at the crater, although the two sources are not well discriminated from each other at Sakurajima (Uhira *et al*., 1995). Harmonic tremors sometimes follow explosion earthquakes one to eight minutes after the onset of explosions, and these tremors are interpreted to be caused by the resonance of bubbly magma in the uppermost part of the conduit. In this case, the conduit opened partially (Maryanto *et al*., 2008).

## 7.  Conclusions and future considerations

At the Sakurajima volcano, where three representative eruptions occurred in the 20th century, a magma plumbing system has been extensively investigated. The main magma reservoir is located at a depth of 10 km beneath the center of the Aira caldera, and the minor magma reservoir located at a depth of from 3 to 6 km beneath the central cone of Sakurajima is directly related to the eruptive activity of the Minamidake crater. The minor reservoir is connected to the crater bottom of the Minamidake by the conduit. Magma supply systems inferred from seismic and geodetic observations are schematically summarized in Fig. 18. Magma is supplied to the main reservoir at a rate of $10^7$ m$^3$/year. High and low eruptivities correspond to deflation and inflation of the reservoir, respectively.

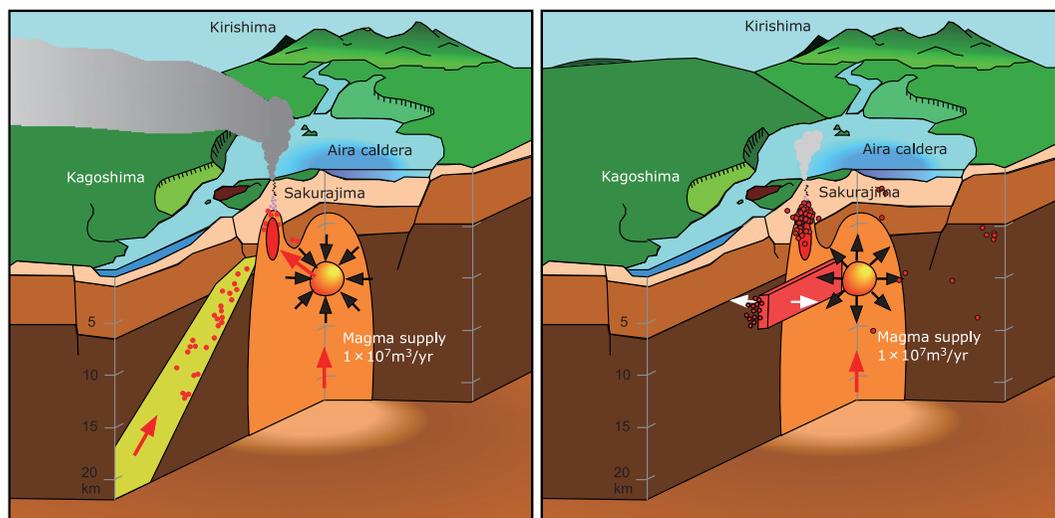The ascent of magma through the conduit and the

Fig. 18.　Image of magma supply beneath the Sakurajima volcano. (a) 1974−1992 (modified from Kamo, 1988) when vulcanian eruptions reoccurred at the Minamidake crater. (b) after 1993 (modified from Hidayati *et al*., 2007) when the eruptive activity decreased.

subsequent intrusion induces a sequence of BL-type earthquake swarms and explosive eruptions.  The cap rock and the gas pocket immediately beneath the cap rock at the top of the conduit increases the pressure in the conduit and triggers an explosion by minor pressure decrease to start sudden formation of gas bubbles.

　　The magma path remains an unresolved problem.  The major pressure source remains near the center of the Aira caldera.  However, the inflation source is located significantly to the west of the deflation source, considering the high density of the leveling benchmarks in northern Sakurajima.  In addition, the inferred magma path at the north and northeastern parts of Sakurajima is the lowest seismic zone in and around Sakurajima.

　　In June 2006, the eruptive activity at the Showa crater resumed after 58 years of dormancy, and the eruptive activity has gradually increased.  However, the seismicity of volcanic earthquakes and ground deformation remained at a lower level compared with the previous period treated in this review.  More precise and dense seismic and geodetic observations, a survey on the internal structure of the volcano and its temporary change, and quasi-real-time monitoring of eruptive material are required to prepare for future eruption.

**References**

Abe, K. (1981) Seismometrical re-evaluation of the Sakurajima Earthquake of January 12, 1914. *Geophys. Bull. Hokkaido Univ.*, **39**, 57−62 (in Japanese with English abstract).

Eto, T. and Nakamura, S. (1986) Ground deformation around Sakurajima volcano −1974〜1982−. In *Report on 5th joint observation of Sakurajima volcano*, 11−21 (in Japanese).

Eto, T., Takayama, T., Yamamoto, K., Hendrasto, M., Miki, D., Sonoda, T., Matsushima, K., Uchida, K., Yakiwara, H., Wan, Y., Kimata, F., Miyajima, R. and Kobayashi, K. (1997) Re-upheaval of the ground surface at the Aira caldera −December 1991〜October 1996−. *Ann. Disast. Prev. Res. Inst., Kyoto Univ.*, **40B-1**, 49−60 (in Japanese with English abstract).

Eto, T., Takayama, T., Yamamoto, K., Hendrasto, M., Miki, D., Sonoda, T., Matsushima, K., Uchida, K., Yakiwara, H., Wan, Y., Kimata, F., Miyajima, R. and Kobayashi, K. (1998a) Result of precise leveling around Sakurajima volcano −December 1991〜October 1996−. In *Report on 9th joint observation of Sakurajima volcano*, 15−29 (in Japanese).

Eto, T., Takayama, T., Sonoda, T. and Yamamoto, K. (1998b) Result of EDM around Sakurajima volcano −January 1992〜December 1996−. In *Report on 9th joint observation of Sakurajima volcano*, 31−37 (in Japanese).

Hagiwara, T., Omote, S., Murauchi, S., Akashi, K. and Yamada Z. (1948) The eruption of Mt. Sakura-Zima in 1946. *Bull. Earthq. Res. Inst., Univ. Tokyo*, **24**, 143−159 (in Japanese with English abstract).

Hashimoto, M. and Tada, T. (1988) Crustal movements

associated with the 1914 eruption of Sakurajima volcano, Kagoshima, Japan. In *Proceedings Kagoshima international conference on volcanoes* 1988, 288–291.

Hidayati, S., Ishihara, K. and Iguchi, M. (2007) Volcano-tectonic earthquakes during the stage of magma accumulation at the Aira caldera, southern Kyushu, Japan. *Bull. Volcanol. Soc. Japan*, **52**, 289–309.

Iguchi, M. (1989) Distribution of the initial motions of volcanic microearthquakes (B-type) at Sakurajima volcano. *Ann. Disast. Prev. Res. Inst., Kyoto Univ.*, **32B-1**, 13–22 (in Japanese with English abstract).

Iguchi, M. (1994) A vertical expansion source model for the mechanisms of earthquakes originated in the magma conduit of an andesitic volcano: Sakurajima, Japan. *Bull. Volcanol. Soc. Japan*, **39**, 49–67.

Iguchi, M. (2006) Aira caldera storing magma. *Chikyu Monthly*, **28**, no.2, 115–121 (in Japanese).

Iguchi, M., Ishihara, K. and Kamo, K. (1983) On ejection velocity and pressure of volcanic explosion reduced from photo-trajectory of volcanic bombs. *Ann. Disast. Prev. Res. Inst., Kyoto Univ.*, **26B-1**, 9–13 (in Japanese with English abstract).

Iguchi, M., Takayama, T., Yamazaki, T., Tada, M., Suzuki, A., Ueki, S., Ohta, Y. and Nakao, S. (2008a) Movement of Magma at Sakurajima Volcano Revealed by GPS Observation. *Ann. Disast. Prev. Res. Inst., Kyoto Univ.*, **51B**, 241–246 (in Japanese with English abstract).

Iguchi, M., Yakiwara, H., Tameguri, T., Hendrasto, M. and Hirabayashi, J. (2008b) Mechanism of explosive eruption revealed by geophysical observations at the Sakurajima, Suwanosejima and Semeru volcanoes. *Jour. Volcanol. Geotherm. Res.*, **178**, 1–9.

Ishihara, K. (1981) A quantitative relation between the ground deformation and the volcanic materials ejected. Abstract 1981 IAVCEI Symposium–Arc Volcanism, 143.

Ishihara, K. (1985) Dynamical analysis of volcanic explosion. *Jour. Geodyn.*, **3**, 327–349.

Ishihara, K. (1988) Geophysical evidences on the existence of magma reservoir and conduit at Sakurajima volcano, Japan. *Ann. Disast. Prev. Res. Inst., Kyoto Univ.*, **31B-1**, 59–73 (in Japanese with English abstract).

Ishihara, K. (1990) Pressure sources and induced ground deformation associated with explosive eruptions at an andesitic volcano: Sakurajima volcano, Japan. In *Magma transport and storage* (Ryan, M. P. ed), 335–356, John Wiley & Sons.

Ishihara, K. and Eto, T. (1978) Surface deformation associated with the eruptive activity at the summit crater of Sakurajima volcano. *Ann. Disast. Prev. Res. Inst., Kyoto Univ.*, **21B-1**, 152–162 (in Japanese with English abstract).

Ishihara, K. and Iguchi, M. (1989) The relationship between micro-earthquake swarms and volcanic activity at Sakurajima volcano. *Ann. Disast. Prev. Res. Inst., Kyoto Univ.*, **32B-1**, 1–11 (in Japanese with English abstract).

Ishihara, K., Takayama, T., Tanaka, Y. and Hirabayashi, J. (1981) Lava flows at Sakurajima volcano (1) Volume of the historical lava flows. *Ann. Disast. Prev. Res. Inst., Kyoto Univ.*, **24**, 1–10 (in Japanese with English abstract).

Ishikawa, H., Eto, T., Tanaka, Y. and Ueki, S. (1981) Chronology of eruptive activity of Sakurajima volcano. In *Report on Grant-Aid No.A-56-1*, 153–179 (in Japanese).

Kamo, K. (1978) Some phenomena before the summit eruptions at Sakura-zima volcano. *Bull. Volcanol. Soc. Japan*, **23**, 53–64 (in Japanese with English abstract).

Kamo, K. (1988) A dialogue with Sakurajima volcano. In *Proceedings Kagoshima international conference on volcanoes* 1988, 3–11.

Kamo, K. and Ishihara, K. (1989) A preliminary experiment on automated judgment of the stages of eruptive activity using tiltmeter records at Sakurajima, Japan. In *Volcanic hazards* (Latter, J. H. ed.), IAVCEI Proceedings in Volcanology 1, 585–598, Springer-Verlag.

Kamo, K., Furuzawa, T. and Akamatsu, J. (1977) Some natures of volcanic micro-tremors at the Sakura-jima volcano. *Bull. Volcanol. Soc. Japan*. **22**, 41–58 (in Japanese with English abstract).

Kamo, K., Nishi, K., Takayama, T. and Ueki, S. (1980) Seismicity south off Sakurajima and anomalous areas of propagation of seismic wave. In *Report on 3rd joint observation of Sakurajima volcano*, 11–15 (in Japanese).

Kanamori, H., Given, J. W. and Lay, T. (1984) Analysis of seismic body waves excited by the Mount St. Helens eruption of May 18, 1980. *J. Geophys. Res.*, **89**, 1856–1866.

Kriswati, E. and Iguchi, M. (2003) Inflation of the Aira caldera prior to the 1999 eruptive activity at Sakurajima volcano detected by GPS network in south Kyushu. *Ann. Disast. Prev. Res. Inst., Kyoto Univ.*, **46B**, 817–826.

Maryanto, S., Iguchi, M. and Tameguri, T. (2008) Constraints on source mechanism of harmonic tremor based on seismological, ground deformation and visual observations at Sakurajima Volcano, Japan. *Jour. Volcanol. Geotherm. Res.*, **170**, 198–217.

Minakami, T. (1974) Seismology and volcanoes in Japan. In *Physical volcanology* (Civetta, L., Gasparini, P., Luongo, G., Rapolla, A., eds), 1–27, Elsevier.

Miyabe, N. (1934) Deformation of earth's crust in the neighborhood of Sakurazima. *Bull. Earthq. Res. Inst., Univ. Tokyo*, **12**, 471–481 (in Japanese with English abstract).

Mogi, K. (1958) Relation between the eruptions of various volcanoes and the deformations of the ground surface around them. *Bull. Earthq. Res. Inst., Univ. Tokyo*, **36**, 99–134.

Nishi, K. (1976) On the explosion earthquake of Sakurajima volcano. *Ann. Disast. Prev. Res. Inst., Kyoto Univ.*, **19B-1**, 69–73 (in Japanese with English abstract).

Nishi, K. (1978) On the focal mechanism of volcanic earthquakes at Sakurajima volcano. *Ann. Disast. Prev. Res. Inst., Kyoto Univ.*, **21B-1**, 145–152 (in Japanese with English abstract).

Nishi, K. (1984) Volcanic B-type earthquake swarm preceding volcanic explosion. *Ann. Disast. Prev. Res. Inst., Kyoto Univ.*, **27B-1**, 29–34 (in Japanese with English abstract).

Nagata, T., Asada, T. and Suzuki, Z. (1948) Volcanic tremors

of short periods at the eruption of Sakura-jima. *Bull. Earthq. Res. Inst., Univ. Tokyo*, **24**, 185‒192 (in Japanese with English abstract).

Nogami, K., Iguchi, M., Ishihara, K., Hirabayashi, J. and Miki, D. (2006) Behavior of fluorine and chlorine in volcanic ash of Sakurajima volcano, Japan in the sequence of its eruptive activity. *Earth Planets Space*, **58**, 595‒600.

Omori, F. (1916) The Sakura-Jima eruptions and earthquakes, II. *Bull. Imp. Earthq. Inv. Comm.*, **8** (6), 179p.

Ono, K., Ito, K., Hasegawa, I., Ichikawa, K., Iizuka, S., Kakuta, T. and Suzuki, H. (1978): Explosion seismic studies in south Kyushu especially around the Sakurajima volcano. *J. Phys. Earth*, **26**, s309-s319.

Sassa, K. (1956) A few problems on prediction of earthquake (II). In *Proceedings of the fifth anniversary of founding of Disast. Prev. Res. Inst. Kyoto Univ.*, 3‒7 (in Japanese).

Suzuki, T. (1999) Detection of anomalous propagation of P-wave at a shallow part of Sakurajima volcano by using after-shocks of 1997 NE Kagoshima Earthquake. Master Thesis of Kyoto Univ. (in Japanese).

Tameguri, T., Iguchi, M. and Ishihara, K. (2002) Mechanism of explosive eruptions from moment tensor analyses of explosion earthquakes at Sakurajima volcano, Japan. *Bull. Volcanol. Soc. Japan*, **47**, 197‒215.

Tameguri, T., Maryanto, S. and Iguchi, M. (2007) Source mechanisms of harmonic tremors at Sakurajima Volcano. *Bull. Volcanol. Soc. Japan*, **52**, 273‒279 (in Japanese with English abstract).

Tateo, Y. and Iguchi, M. (2009) Ground deformation associated with BL-type earthquake swarms at Sakurajima volcano. *Bull. Volcanol. Soc. Japan*, **54**, 175‒186 (in Japanese with English abstract).

Tsuboi, C. (1929) Block movements as revealed by means of precise levellings in some earthquake districts of Japan. *Bull. Earthq. Res. Inst., Univ. Tokyo*, **7**, 103‒114.

Tsuya, H. and Minakami, T. (1940) Minor activity of volcano Sakura-zima in October, 1939. *Bull. Earthq. Res. Inst., Univ. Tokyo*, **18**, 318‒339 (in Japanese with English abstract).

Uhira, K. and Ueda, Y. (1988) Volcano monitoring at Kagoshima Local Meteorological Observatory of the Japan Meteorological Agency. In *Proceedings Kagoshima international conference on volcanoes* 1988, 227‒229.

Uhira, K. and Takeo, M. (1994) The source of explosive eruptions of Sakurajima volcano, Japan. *J. Geophys. Res.*, **99**, 17,775‒17,789.

Uhira, K., Ikeda, S. and Takeo, M. (1995) Source process of explosion earthquakes deduced from short-period records at Sakurajima volcano. *Bull. Volcanol. Soc. Japan*, **40**, 295‒310.

Yamakawa, N. (1955) On the strain produced in a semi-infinite elastic solid by an interior source of stress. *J. Seismol. Soc. Japan*, **8**, 84‒98 (in Japanese with English abstract).

Yamamoto, K., Takayama, T., Yamazaki, T., Tada, M., Ohkura, T., Yoshikawa, S., Matsushima, T., Uchida, K., Nakamoto, M., Hiraoka, Y., Shioya, T. and Nemoto, M. (2008) Precise leveling survey around Sakurajima volcano (October‒December 2007). In *Report on 10th joint observation of Sakurajima volcano*, 45‒51 (in Japanese).

Yamamoto, K., Sonoda, T., Takayama, T., Ichikawa, N., Ohkura, T., Yoshikawa, S., Inoue, H., Matsushima, T. and Uchida, K. (2010) Precise leveling surveys in and around Sakurajima volcano (November 2009 and April 2010). In *Report on Integrated volcano observation for the study on preparation process of eruption at Sakurajima volcano* (Iguchi, M. ed.), 41‒46 (in Japanese with English abstract).

Yamasato, H. (1987) Distribution of the initial motions of explosion earthquakes at Sakurajima volcano. *Bull. Volcanol. Soc. Japan*, **32**, 289‒300 (in Japanese with English abstract).

Yamasato, H. (2005) Modern history of volcano observation in Japan ‒Especially volcano surveillance of Japan Meteorological Agency‒. *Bull. Volcanol. Soc. Japan*, **50**, Special Issue, S7-S18 (in Japanese with English abstract).

Yokoo, A. and Ishihara, K. (2007) Analysis of pressure waves observed in Sakurajima eruption movies. *Earth Planets Space*, **59**, 177‒181.

Yokoo, A., Tameguri, T. and Iguchi, M. (2009) Swelling-up of lava plug associated with Vulcanian eruption at Sakurajima volcano, Japan, as revealed by infrasound record‒Case study on eruption on January 2, 2007‒. *Bull. Volcanol.*, **71**, 619‒630.

Yokoyama, I. (1986) Crustal deformation caused by the 1914 eruption of Sakurajima volcano, Japan and its secular changes. *Jour. Volcanol. Geotherm. Res.*, **30**, 283‒302.

Yoshikawa, K. (1961) On the crustal movement accompanying with the recent activity of the volcano Sakurajima (Part 1). *Bull. Disast. Prev. Res. Inst., Kyoto Univ.*, **48**, 1‒15.

(Editorial handling Takeshi Nishimura)

# 地球物理学的観測によって明らかになった桜島火山の深部から浅部へのマグマの動き

## 井口正人

　地震観測と地盤変動観測に基づいて 1914 年，1946 年，1955 年以降と 3 つの特徴的な噴火が発生した桜島火山におけるマグマ供給系とマグマの動きに関する研究について総説する．桜島のマグマ供給系は桜島の北方，姶良カルデラの地下約 10 km にあると推定される深部マグマ溜り，中央火口丘下の深さ 3～6 km の浅部マグマ溜りおよび南岳山頂火口につながる火道から構成される．上下変動の空間分布と時間変化から，年間 $10^7 \mathrm{m}^3$ のマグマが深部溜りに供給されてきた．浅部溜りは，地盤の上下変動，爆発的噴火直前の火口方向の隆起の傾斜変化や地震波の異常減衰域の存在から推定される．姶良カルデラの隆起に続く桜島への隆起中心の移動と火山性地震の震源の深部から南岳直下の浅部へ移動は中央火口丘下へのマグマの移動・上昇に対応する．中央火口丘下のマグマ溜まりと火口底をつなぐ火道の存在とその大きさをせん断破壊により発生する A 型地震と体積膨張に伴う B 型・爆発地震の震源位置の違いから推定できる．火道内をマグマがスムーズに上昇して火口底に達した時は，BL 型地震を伴うストロンボリ式噴火が発生し，脱ガスしたマグマが火道上部に蓋とガス溜まりを形成している状態でマグマが貫入してきたときはブルカノ式噴火が発生する．いずれの場合も火口周辺の地盤の隆起と伸長が観測され，噴火の発生とともに沈降，収縮へ反転する．マグマの揮発性成分は火道上部のガス溜りの形成と火山ガスの漏洩に伴う圧力低下によって引き起こされるマグマの急激な発泡に重要な役割を果たす．